Current challenges and opportunities towards understanding hydrogen embrittlement mechanisms in advanced high-strength steels

Authors: Binhan Sun[1], Dong Wang[2], Xu Lu[2], Di Wan[2], Dirk Ponge[1], Xiancheng Zhang[3]

Affiliations:

[1]Max-Planck-Institut für Eisenforschung GmbH, Max-Planck-Straße 1, 40237 Düsseldorf, Germany.

[2]Department of Mechanical and Industrial Engineering, Norwegian University of Science and Technology, Richard Birkelands vei 2B, 7491 Trondheim, Norway.

[3]Key Laboratory of Pressure Systems and Safety, Ministry of Education, School of Mechanical and Power Engineering, East China University of Science and Technology, 200237, Shanghai, China.

Abstract: Hydrogen embrittlement (HE) is one of the most dangerous yet most elusive embrittlement problems in metallic materials. Advanced high-strength steels (AHSS) are particularly prone to HE, as evidenced by the serious degradation of their load-bearing capacity with the presence of typically only a few parts-per-million H. This strongly impedes their further development and application, and could set an abrupt halt for the weight reduction strategies pursued globally in the automotive industry. It is thus important to understand the HE mechanisms in this material class, in order to develop effective H-resistant strategies. Here we review the related research in this field, with the purpose to highlight the recent progress, and more importantly, the current challenges towards understanding the fundamental HE mechanisms in modern AHSS. The review starts with a brief introduction of current HE models, followed by an overview of the state-of-the-art micromechanical testing techniques dedicated for HE study. Finally, the reported HE phenomena in different types of AHSS are critically reviewed. Focuses are particularly placed on two representative multiphase steels, i.e. ferrite-martensite dual-phase steels and ferrite-austenite medium-Mn steels, with the aim to highlight the multiple dimensions of complexity of HE mechanisms in complex AHSS. Based on this, open scientific questions and the critical challenges in this field are discussed to guide future research efforts.

1. Introduction

Hydrogen embrittlement (HE) corresponds to the abrupt loss of a material's load-bearing capacity or damage resistance in presence of H. This phenomenon was firstly documented by Johnson in 1875 [1] and has been observed in many metallic materials including iron and steels, Ti alloys, Al alloys and superalloys [2-9]. Since the H ingress into a material is normally difficult to avoid due to the ubiquitous nature of H atoms, HE is a particularly dangerous embrittling phenomenon and often responsible for catastrophic and unpredictable failure of large-scale engineering structures [5, 10]. The concern to HE has thus triggered a considerable amount of studies in the past more than 100 years.

Among all the alloy classes, advanced high-strength steels (AHSS) are particularly prone to HE [5, 11-13]. These steels are continuously sought after in the automotive industry, in order to meet the body-in-white weight reduction strategies for fuel economy and vehicle safety. However, the ingress of typically only a few parts-per-million H can result in a serious degradation of strength and/or ductility in certain AHSS grades [11, 14]. H uptake in these materials can occur in various stages of manufacturing (steelmaking processes and car body manufacturing) as well as in service. In the former case, the embrittlement is often induced by internal H, which manifests itself by the delayed fracture phenomenon typically after sheet forming. In the service life of a vehicle, H normally enters into the steel when the protective layer is damaged and exposed to a wet/corrosive atmosphere. In this scenario, the failure caused by H is also referred to as external HE.

Despite extensive investigations over the last 100 years, HE is still an unsolved issue. In particular, its fundamental embrittling mechanisms have not been understood even in single-phase model alloys [8, 15-17]. A variety of embrittlement models caused by atomic H have been proposed, including hydrogen-enhanced decohesion (HEDE) [17], hydrogen-enhanced localized plasticity (HELP) [8], HEDE and HELP synergistic effect [18], hydrogen-enhanced strain-induced vacancies (HESIV) [19], adsorption-induced dislocation emission (AIDE) [20] and Defactant concept [21]. Strong disagreement and polarized opinions generally exist among these models and their interplay. On the other hand, modern AHSS often possess a complex microstructure consisting of multiple phases and deformation behavior involving complex defect evolution and stress/strain localization [12, 22-27]. The change of microstructure and deformation behavior

could alter the prevalent HE mechanisms and significantly influence the mechanical response in the presence of H. Although it is of great importance to visualize the full picture of HE in AHSS, the task is rather challenging given the great complexity in both HE itself and in the material class. This review is thus to highlight the most critical problems/challenges for understanding HE mechanisms in AHSS, with the intention to promote future research efforts. The review starts from a brief description about relevant HE mechanisms that might occur in AHSS. Then some state-of-the-art micromechanical testing methods dedicated to HE investigations are overviewed. At last, the HE problems and mechanisms in two representative multiphase steels, i.e. ferrite-martensite dual-phase (DP) steels and ferrite-austenite medium-Mn steels are critically reviewed, with the aim to highlight the multiple dimensions of complexity of HE mechanisms in complex AHSS.

2. Fundamental hydrogen embrittlement models

2.1 Hydrogen-enhanced decohesion (HEDE)

In the H-enhanced decohesion model, it is proposed that the presence of H decreases the cohesive strength of lattice planes or interface boundaries [28, 29]. The underlying mechanism, suggested by Troiano [29], is that the electron of the H atom tends to enter the unfilled 3d shell of the iron atoms, which then increases the interatomic repulsive forces thus decreasing the cohesive strength. However, the solubility of H in many metals is probably too low (e.g. 0.7 at ppm inside ferritic stainless steels at 1 atm gaseous H atmosphere and room temperature [30]) to result in a significant decohesion effect, if H atoms are homogenously distributed in the microstructure. Therefore, an important assumption for this model is that a sufficiently high H concentration needs to be accumulated at the sharp crack tip region caused by the hydrostatic stress field, which continuously weakens the interatomic bonds ahead of the crack tip [28, 31, 32]. The existence of very high concentrations of H near a crack tip has indeed been experimentally measured or modeled by some researchers [33-35]. The simulation results from Gerberich et al. [31] showed that in pure iron the elastic stress can reach up to 20,000 MPa (near the theoretical stress of the material) at 23 nm in front of the crack tip, due to a dislocation shielding effect. Such a high stress level should be sufficient to attract H to render the decohesion effect [31]. This assumption is also consistent with the fact that the degree of HE is normally strain-rate dependent and the existence of a slow propagation stage of H-induced cracks before catastrophic failure [29]. The frequently reported embrittling sites due to the HEDE mechanism are grain boundaries or interphase boundaries [13,

17], leading to an intergranular typed fracture surface. However, it has been questioned that whether H alone can cause interface decohesion, as other harmful elements such as Mn, S, P and Si can also segregate at these locations [36, 37]. Therefore, a combined effect of H and these embrittling elements on intergranular fracture has been proposed by some researchers [17]. Nevertheless, although a direct experimental evidence for the decreasing effect of H on cohesive energy is difficult to acquire, this point has been supported by numerous simulation works [38, 39]. For example, Jiang et al. [38] have calculated the ideal fracture energy (twice the surface energy) of (111) plane in Al and (110) plane in Fe using density functional theory (DFT) and found an almost linearly decreasing trend of the fracture energy as a function of H coverage. Similar behavior has also been found in the work of Alvaro et al. [4] for Coincident Lattices Sites (CLS) Σ3 and Σ5 grain boundaries. Tahir et al. [40] have shown that even when the grain boundary is segregated by the cohesion-enhancing element C, the presence of H still decreases interface cohesion due to the detrimental mechanical contribution of H and a H-induced decrease in the beneficial chemical contribution of C atoms. Yamaguchi et al. [32] have further demonstrated using first-principles calculations that the reduction in the grain boundary cohesive energy is more influenced by the mobile H segregated to the newly formed crack surface.

2.2 Hydrogen-enhanced local plasticity (HELP)

The H-enhanced local plasticity mechanism was firstly suggested by Beachem [41] in 1971, based on the fracture surface analysis as a function of stress intensity factor in quenched and tempered steels and a comparison of the flow stresses in atmospheres with and without H. This model was then further developed by Birnbaum, Robertson and other researchers [9, 42, 43] based on elasticity theory and a series of *in-situ* transmission electron microscopy (TEM) observations. According to linear elasticity and finite element calculations [42, 43], H can provide a shielding effect which reduces the repulsive force acting between edge dislocations and other obstacles (e.g. other parallel edge dislocations with Burgers vectors of the same sign, precipitates and interfaces). Such reduction is associated with the volumetric strain induced by H entering the lattice and the H-induced change of the constitutive moduli [9, 42]. It should be noted that the H shielding effect is only manifest when the dislocations move with the H atmospheres formed around them. Atomic simulations of H-dislocation interactions have also provided some insights on the underlying mechanisms of H-enhanced dislocation mobility, especially for the behavior of screw dislocations

[44, 45]. It has been calculated by DFT that the presence of H can decrease the core energy and Peierls potential for both edge and screw dislocations in iron [44]. Itakura et al. [45] also showed an increasing screw dislocation velocity in iron for certain temperature ranges based on their first-principles calculation, which was due to the reduction of kink nucleation energy. However, different opinions emerged regarding whether H indeed increases the dislocation mobility. Song and Curtin [46, 47] have conducted a series of molecular dynamics calculations and shown that the H Cottrell atmospheres do not shield the interactions between edge dislocations in iron but rather suppress their motion. This point was recently supported by Xie et al. [48] who studied H-dislocation interaction in single crystal Al using *in-situ* TEM nanocompression tests. They further claimed that the observed decreased mobility of dislocation caused by H was due to the locking effect of the formation of superabundant hydrogenated vacancies [48].

Nevertheless, the calculations based on elasticity theories successfully predict an increased mobility of dislocations upon loading (thus an enhanced plasticity) and a smaller equilibrium spacing between pileup dislocations in the presence of H, which have indeed been observed in various metals [9, 49-51]. In this regard, the concentrated H near the tips of either brittle or ductile cracks will produce a highly localized plastic zone, which makes the materials readily achieve the plasticity limit and promotes the formation of damages (Fig. 1) [9, 16]. Therefore, the failure induced by this mechanism is intrinsically a ductile fracture mode which might occur in confined zones in the absence of macroscopic deformation (i.e. macroscopically 'embrittlement'). Further experimental evidence supporting this mechanism includes (a) sometimes observed lower flow stresses in the presence of H compared with H-free specimens [9, 41, 42], (b) shallower dimples in the H-charged and fractured samples compared with the case in the absence of H [13], and (c) a higher density of dislocations just underneath the scanning electron microscope (SEM)-resolved H-induced cleavage or intergranular facets [8], observed by TEM performed on focused ion beam (FIB)-prepared specimens. It is important to mention that these results on bulk materials only provide indirect insights for the HELP mechanism. A direct evidence linking the H-enhanced plasticity and damage formation is still lacking.

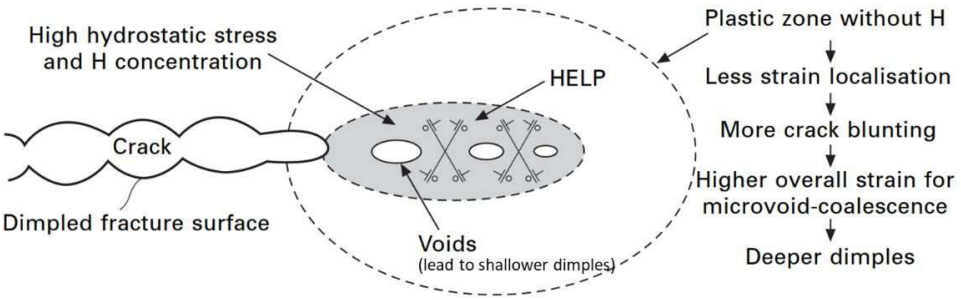

Fig. 1 Schematic diagram showing the failure mechanism induced by the HELP model. (Reprinted with permission from Ref. [20]).

2.3 Adsorption-induced dislocation emission (AIDE)

Sufficient evidence has shown that H atoms are easily absorbed at free surfaces and sub-surface sites [52, 53]. The adsorption-induced dislocation emission (AIDE) model, proposed by Lynch et al. [20], thus highlights the effects of surface-absorbed H on promoting dislocation emission at the surface. It is essentially a model describing the interaction between surface (either internal cracks or voids or free specimen surfaces) and H atoms (either internal diffusible H or environmental H). Unlike the HELP-associated failure mechanism where the crack propagation is promoted by the enhanced dislocation mobility close to the crack tip, the AIDE model proposes that it is the enhanced dislocation emission at the crack surface which produces crack advance (Fig. 2 [16]). Theoretical calculations have shown that H should not diffuse for more than a few atomic distances when the ratio between H diffusivity D and crack propagation velocity v, D/v, is below ~10^{-8} cm [54]. However, HE can still occur at such 'high' crack velocity. This is similar to the case of liquid-metal embrittlement (LME) where solute adsorption must occur at crack tips. Such similarity, along with other similar fractographic features between HE and LME [16, 20], provide a support for the operation of AIDE in H-induced failure.

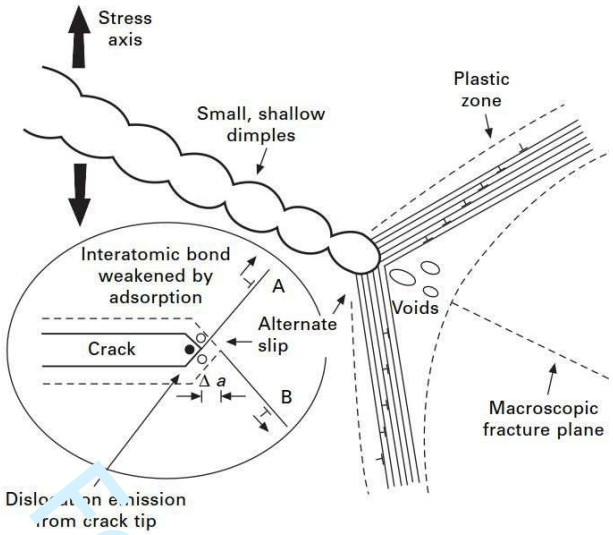

Fig. 2 Schematic diagram showing the failure mechanism induced by the AIDE model (Δa, the length of the crack growth). (Reprinted with permission from Ref. [20]).

2.4 Hydrogen-enhanced strain-induced vacancies (HESIV)

The H-enhanced strain-induced vacancies (HESIV) or H-induced superabundant vacancies model was built based on thermal desorption spectrometry (TDS) in iron and low alloyed ferritic steels [55-58]. It was observed that a decrease in H desorption rate occurred below 200˚C at which the dislocation density was not deemed to be changed [55, 56]. Such reduction was then proposed to be the result of the annihilation of vacancies [55, 56]. Nagumo et al. [55-57] further found that the density of strain-induced vacancies deduced from the TDS data was increased with the presence of H, based on which the HESIV mechanism was proposed. This mechanism was further supported by the positron annihilation spectroscopy (PAS) where the mean positron lifetime in iron was found to be increased by tensile straining and such increase was further enhanced in the presence of pre-charged H [59]. The stabilization of vacancies due to H is also consistent with the framework of the defactants (DEFect ACTing AgeNTS) concept [60] which will be described in **Section 2.5**. The H-induced superabundant vacancies would promote the formation of vacancy clusters and very small nano-sized voids, which could result in a premature fracture near the high stress/strain concentrators (e.g. crack tips). Neeraj et al. [61] have conducted careful SEM analysis on fracture surfaces in H-charged and embrittled ferritic pipeline steels. Using high surface resolution SEM parameters (3~7 kV operating voltage and 3~5 mm working distance), they found that the brittle facet that was normally observed in a lower magnification showed a “mottled” dark-

bright contrast on the nano-scale (Figs. 3 (a) and (b)). Such contrast was suggested to correspond to nano-dimples which was supported by a careful observation of the conjugate fracture surfaces and the atomic force microscopy (AFM) results (Fig. 3 (c)). The presence of nano-dimples was then a sign of the operation of the HESIV model. However, more direct experimental evidence for this mechanism will be difficult to acquire, as both vacancies and H are extremely difficult to directly probe using current characterization techniques.

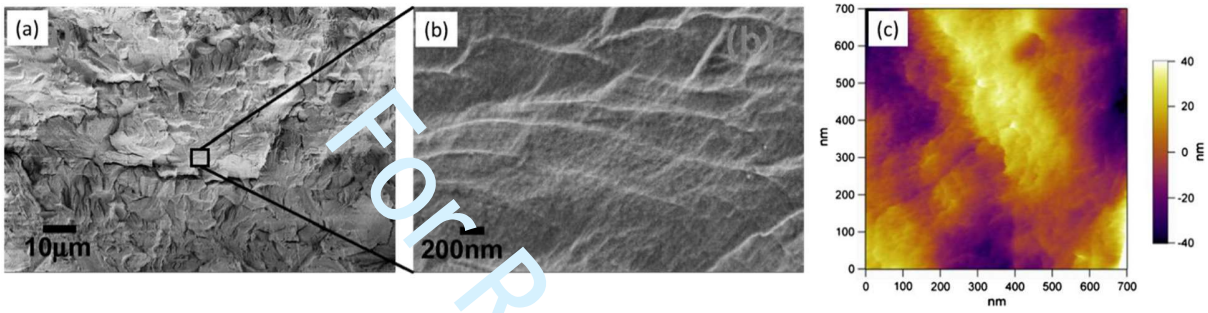

Fig. 3 (a) Fracture surface of H pre-charged and fractured X65 pipeline steel; (b) Higher magnification view of the area marked in (a); (c) Atomic force microscopy (AFM) topography image from a 'brittle' facet in the fracture surface of the same specimen. (Reconstructed with permission from Ref. [61]).

2.5 Defactants concept

The defactants concept, introduced by Kirchheim [60] in 2009, is also a model dealing with the interaction between H and defects (e.g. dislocations and vacancies). It is proposed that H, act as a defactant, reduces the formation energy of defects in a manner analogous to the case that surfactants reduce the surface energy of liquids [21, 62, 63]. The relation between defect density ρ (e.g. grain boundary area, dislocation length and vacancies per volume V) and the amount of defactant atoms such as H has been defined as [21, 60, 62]:

$$\Gamma_H \equiv \frac{1}{V}\frac{\partial n_H}{\partial \rho}\bigg|_{V,T,\mu_{H,n_B}}$$

where Γ is excess defactant which is positive, n_H, n_B, T, μ are the number of H atoms, number of solvent atoms, temperature and chemical potential, respectively. This concept thus provides a thermodynamic foundation for the aforementioned HELP, AIDE and HESIV effects, i.e. accelerated generation of dislocations and vacancies due to the segregation of H atoms. It can

explain both the easier nucleation of dislocations which the elasticity theory does not cover [42, 43] and the H-enhanced dislocation mobility driven by the reduction of the formation energy of kink pairs. The former phenomenon was strongly supported by recent nanoindentation tests on coarse grained materials where a clear reduction of pop-in loads was observed for the tests conducted under H compared with the H-free condition [64, 65].

2.6 Summary of hydrogen embrittlement micromechanisms

The above sections (2.1~2.5) only provide a brief description of five fundamental HE mechanisms that might occur in AHSS. More systematic and detailed review for each model can be found elsewhere [8, 17, 19-21]. Other HE mechanisms such as the high-pressure molecular H induced failure (or internal pressure theory) [66] and hydride-induced failure are not covered here, as they only become dominant in specific circumstances, e.g. in the presence of supersaturated H [67] or hydride-forming elements (V, Zr, Nb, Ta and Ti) [68]. The latter mechanism has rarely been reported in steels. Among the aforementioned HE models (Sections 2.1~2.5), only the HEDE mechanism produces a pure brittle failure, while other mechanisms result in an intrinsically ductile failure even though sometimes the SEM-resolved fracture surface might show some brittle-like facets. Despite polarized opinions exist pertaining to the prevalence of different models, they generally do not repel each other and can operate synergistically for the premature fracture of materials. For example, the enhanced dislocation activity due to HELP or AIDE might promote the formation of strain-induced vacancies and activate the HESIV mechanism [20, 61]. The higher density of pileup dislocations due to the HELP effect might facilitate H transport to the obstacles (e.g. grain boundaries) thus promoting the occurrence of the HEDE effect [18]. In view of this, it is thus highly possible that not only one HE mechanism exists especially in complex heterogeneous materials like most AHSS, which will be further discussed in Section 4.

3. Advanced in situ and micromechanical testing techniques for hydrogen embrittlement investigation

The conventional approach to detect H effect is to conduct mechanical tests on a H-charged bulk sample in comparison to an uncharged one. The analysis of the degradation of mechanical properties and fracture behavior provides useful information on the HE phenomena. However, HE

is a complex process that is affected by many intrinsic compositional and microstructural features and extrinsic variables (e.g. loading atmosphere, strain rate, etc.). These large-scale tests are thus not capable to fully reveal the fundamental HE mechanisms. Moreover, the testing on pre-charged sample cannot precisely bridge the H content and mechanical property degradation, due to the uncountable H loss within the dwell time between charging and testing. Therefore, new approaches integrating *in-situ* H charging and small-scale mechanical testing are needed to better clarify the interaction between H and individual constituents in materials.

3.1 Small-scale *in-situ* tensile tests in SEM

The small-scale tensile tests inside SEM provide the opportunity to capture the microstructure and damage evolution through SEM-based techniques such as secondary electron imaging, back-scattered electron imaging, electron backscattered diffraction (EBSD) and electron channeling contrast imaging (ECCI) [69-72]. The tests can be performed for both pre-charged specimens [73-75] and specimens under an *in-situ* charging condition. For the former case, it is difficult to precisely quantify the amount of H during the testing and imaging due to the continuous H outgassing. Also it would be challenging to differentiate whether the possibly probed defect evolution is due to the presence of H or to the H desorption process. The latter was also reported to affect the activity of dislocations [76]. Recently, some novel setups combining *in-situ* H charging (performed using H plasma [77] or electrochemically [78]) and SEM observation have been developed, which opens new possibilities of studying the H effect in a more comprehensive manner. For example, Depover and Wan et al. [74, 79] have shown that the H plasma charging provides the possibility to *in-situ* charge ferritic or dual-phase materials without causing significant damages on the sample surface. By solely comparing the fatigue crack growth path in a same grain under H-free and H plasma conditions, a noticeably higher crack growth rate with a reduced plastic zone in the H-containing environment was documented, which was concluded as the result of the restricted dislocation activities due to the ingression of H [79]. In comparison with the conventional pressurized H gas or electrochemical charging methods, a relatively weak embrittlement effect is normally induced by H plasma charging. The effect is more visible at high tensile deformation levels [74] or under cyclic loading conditions where the H effects can be accumulated [79].

3.2 Nanoindentation testing with *in situ* H-charging

Nanoindentation testing is a method that was originally designed as a hardness measurement tool focusing on small volumes and films [80]. The modern instrumented nanoindentation is capable of testing various mechanical properties such as elastic modulus, fatigue, creep, and scratch resistance [81, 82]. During nanoindentation tests, a load-displacement curve (Fig. 4) in the order of μN-nm is continuously recorded with a high resolution, providing the possibility to detect the interaction between dislocations and H on a nano- or micro-scale. The effect of H on advanced high strength alloys has been studied by performing nanoindentation tests on pre-charged samples [83, 84]. An enhanced hardness was observed due to the solid solution strengthening by dissolved H [84]. However, a surface hydrogen depletion zone will be formed on pre-charged samples during the nanoindentation test, owing to the outgassing diffusion process. This result indicates that the effect primarily originates from the trapped H instead of diffusible H, since the penetration depth is typically in the range of nanometers for a nanoindentation test. Recently, the *in-situ* electrochemical nanoindentation combined with scanning probe microscopy (ECNI-SPM) have been developed (Fig. 5) [65]. This technique integrates nanoindentation tests with *in-situ* H charging to keep a stable and constant surface H concentration. It has shown its advantage in probing the H effect on both the mechanical properties and the discrete events. For the effect of H on mechanical properties, a H-enhanced hardness was detected on several high strength alloys due to the enhanced retarding stress on dislocation motion and the increased lattice friction between H and dislocations [85-87]. The effect of H on elastic behavior can also be simultaneously determined by ECNI technique. For the discrete events, a H-reduced pop-in load was generally reported on many high strength alloys, which was proposed as the result of the H-enhanced homogenous dislocation nucleation caused by a reduced dislocation nucleation energy [64, 65]. Interestingly, it has been detected using ECNI-SPM that only by H-charging, it is able to induce surface deformation and phase transformation due to the H-enhanced internal stress [88-91]. These H-charging induced-surface phenomena thus need to be considered in future studies pertaining to the explanation of HE.

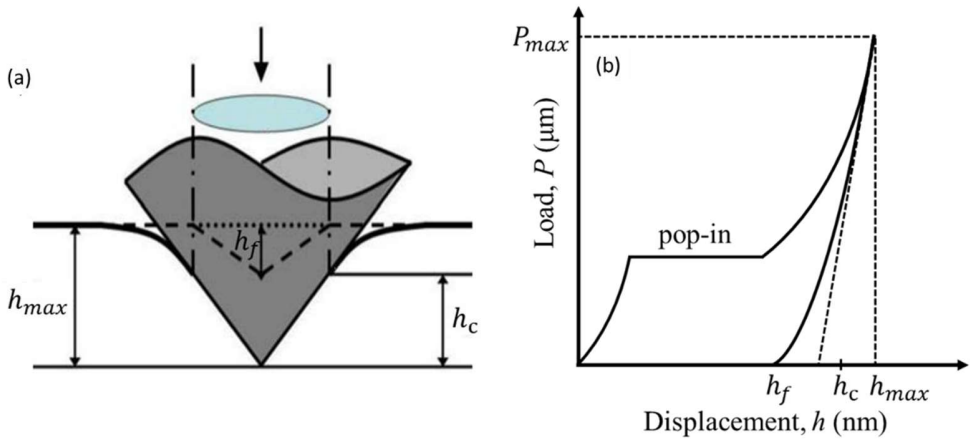

Fig. 4 Schematic drawing of (a) an indentation test at maximum load and (b) the corresponding load-displacement curve.

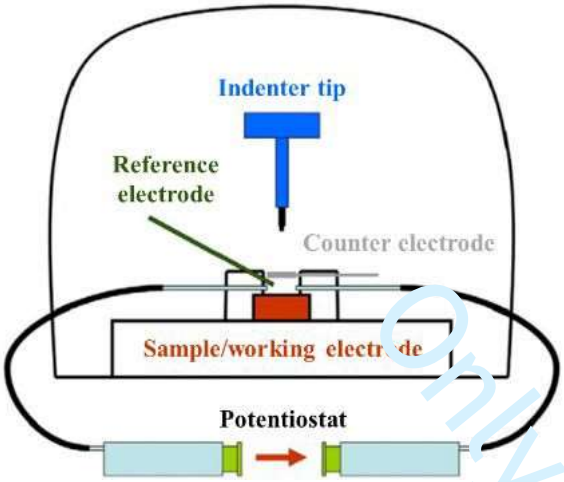

Fig. 5 Schematic drawing of the electrochemical nanoindentation (ECNI) setup. (Reprinted with permission from Ref. [65]).

3.3 Microcantilever bending and pillar compression testing under H atmosphere

Using the similar nanoindentation-based setup, the microcantilever bending and pillar compression test can also be performed with *in-situ* H charging (Figs. 6 and 7). These tests can be carried out in environmental SEM (ESEM) for certain alloys, such as Fe-Al intermetallics where the atomic H was continuously produced by the reaction of aluminum with water vapor used as the environmental condition in ESEM [92]. These micro-scale tests can also be performed in the same electrochemical charging cell as used for ECNI test or in the atmosphere of H plasma.

Moreover, through adding a pre-notch on certain lattice planes of the microcantilevers or milling bi-crystalline micropillars with different types of grain boundaries, a more detailed view of H-assisted cracking along either lattice planes or interfaces can be obtained. These micro-scale testing approaches allow to eliminate the proximity effect from free surface that is always criticized in *in-situ* TEM tests.

The above *in-situ* techniques have been carried out on several alloys, such as nickel-based alloy 725, FeAl, and cantor high-entropy alloys [6, 93]. The results of *in-situ* microcantilever tests on an interstitial CoCrFeMnNi high-entropy alloy (Fig. 6) showed clearly different cracking behavior in H-free (air) and H-charged conditions [93]. In the H-free condition (Fig. 6 (a) and (a_1)), notch blunting accompanied by abundant slip lines (marked by black lines) indicated a ductile fracture mode with a large amount of plasticity during deformation. In contrast, in the H-charged condition (Fig. 6 (b) and (b_1), a sharp cracking and a reduced number of slip lines were observed, elucidating a confined plasticity along the cracking path. Such different cracking behavior in H-free and H-charged conditions was proposed to be due to the synergistic effect of H-enhanced dislocation nucleation and H-reduced dislocation mobility [6, 93]. Fig. 7 shows an example of the *in-situ* bi-crystalline micropillar compression test performed on a solution treated nickel-based Alloy 725 [3]. A H-induced hardening effect was observed from the stress-strain curves, which was attributed to H-enhanced dislocation multiplication and interactions as well as the H-enhanced lattice friction [3]. By adopting transmission-EBSD technique, dislocation behavior along grain boundaries was captured. Transmission-EBSD results on low-angle grain boundary (LAGB) showed a full transmission of dislocations across the grain boundary and relatively homogeneous plastic deformation along micropillars in the H-free condition (Fig. 7 (a)). However, an evident dislocation pile-ups was observed in the H-charged condition (Fig. 7 (b)), indicating a suppression effect of H to dislocation transmission at specific grain boundaries. These results provide valuable insights on the mechanisms of H-induced cracking behavior.

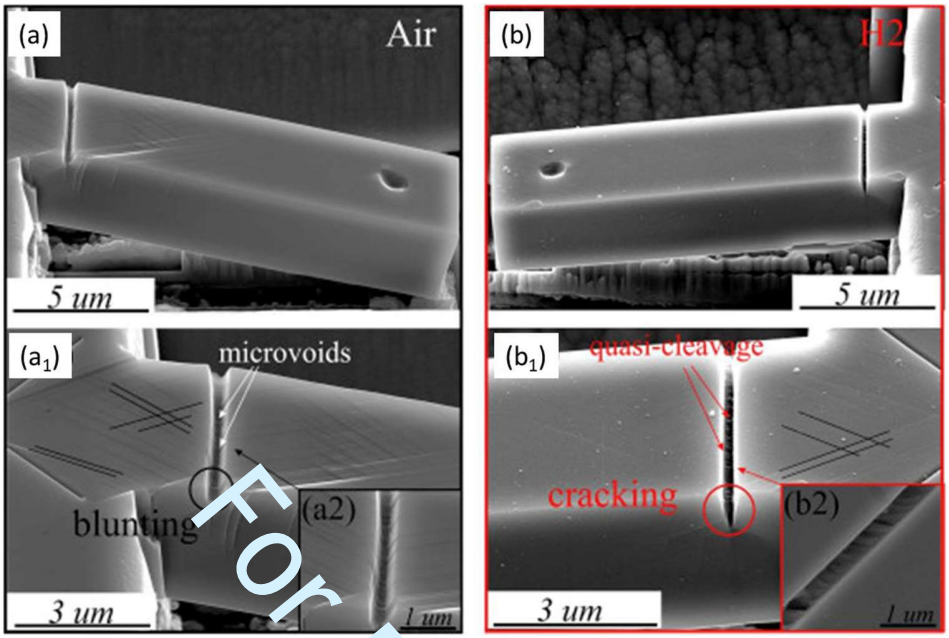

Fig. 6 SEM micrographs showing the deformation behavior of microcantilevers bent in (a)-(a_1) air, and in (b)-(b_1) H atmosphere. (Reprinted with permission from Ref. [93]).

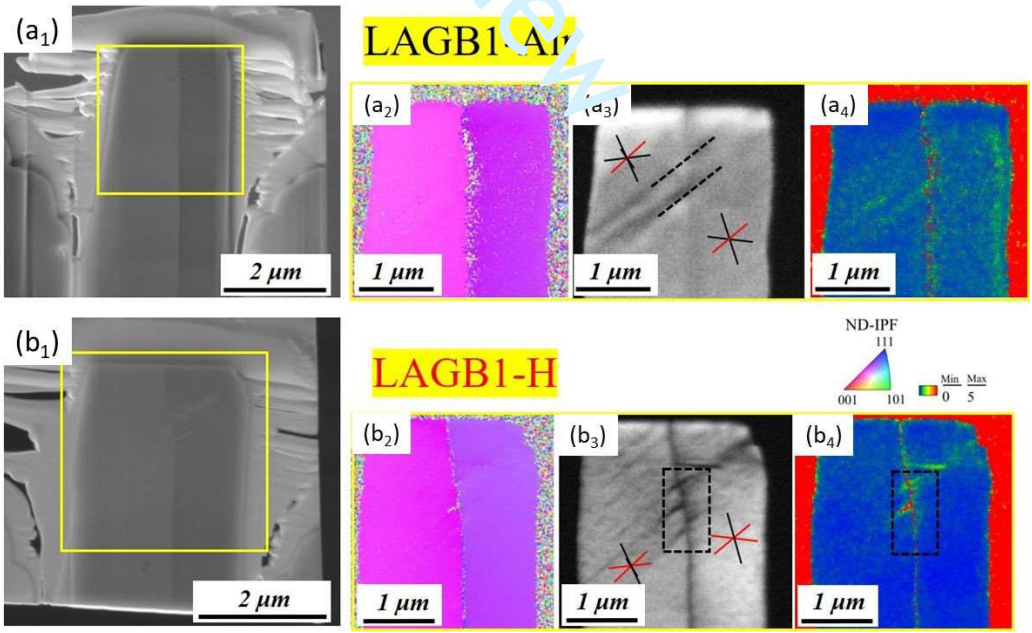

Fig. 7 Micrographs of micropillar lamellae containing a representative low-angle grain boundary (LAGB1) after the compression tests for samples under the (a_1) H-free (air) and (b_1) H-charged conditions. Transmission-EBSD results showing the corresponding (a_2) and (b_2) inverse pole

figures, (a_3) and (b_3) image quality maps, and (a_4) and (b_4) kernel average misorientation (KAM) maps. (Reprinted with permission from Ref. [3]).

3.4 New approaches for charging hydrogen

For the above-mentioned small-scale testing approaches, the choice of H charging method is critical in order to achieve a stable *in-situ* H atmosphere without disturbing the mechanical testing process. Up to now, several "direct" and "indirect" H charging methods have been proposed and are worthwhile to overview. For the "direct" charging method, a glycerol-based solution consisting of borax or phosphorous acid has been widely used for *in-situ* nanoindentation, microcantilever bending, and micropillar compression tests [64, 94]. This electrolyte is appropriate for preserving the sample surface from corrosion throughout the whole testing procedure due to its extremely low solubility and diffusivity of oxygen. It can also provide a high pressure-like surface H due to its high viscosity at room temperature [73]. However, this electrolyte can only be used in ambient atmosphere (normal pressure). For the tests combining with SEM setup, the H plasma charging has been used to provide a mild H source under low vacuum condition [79, 95]. One drawback of such charging method is that the amount of plasma charged H cannot be easily controlled due to the complexity of plasma medium compared with electrochemical charging, where the H can be readily controlled by changing the potential or current. Recently, a new *in-situ* H charging set up was developed, which isolated electrolyte to the backside of sample by a double-wall structured chamber [78]. This setup enables *in-situ* H charging under vacuum condition, such as SEM-based techniques. When H diffuses to the sample surface, simultaneous microstructural observation and micro-mechanical testing can be achieved. As a result, the H-induced microstructural changes can be continuously traced without electrolyte contamination on surface. It needs to mention that this backside charging method is more suitable to metallic materials with BCC lattice structure, which has a much faster H diffusivity than that for FCC structure or BCC-FCC dual-phase structure [13]. The "indirect" charging method can be applied on specific metallic materials that can produce H directly from moisture, such as Fe-Al intermetallics, where atomic H can be produced by the reaction between aluminum and water vapor:

$$2Al + 3H_2O \rightarrow Al_2O_3 + 6H^+ + 6e^-$$

Therefore, given water vapor as the default environment, H-induced cracking can be directly captured using small-scale testing with *in-situ* SEM observation [96].

4. Hydrogen embrittlement in advanced high-strength steels-a critical perspective

The study of HE in AHSS has mainly concentrated on the first and second generations (e.g. high-strength ferritic or martensitic [97], DP [98], transformation-induced plasticity (TRIP) [12] and twinning-induced plasticity (TWIP) [7] steels). Among these studies, most investigated the influence of H charging condition, H content, mechanical and microstructural conditions on the HE susceptibility and H-induced damage characteristics. The active HE mechanisms in these materials, however, are generally less clear. This is partly due to the strong controversies existed among different fundamental HE models, as described in **Section 2**. Further, the extremely fine volume in which H interacts with defects and leads to damages often requires a more careful and higher-resolution characterization beyond SEM-based techniques, which greatly enhances experimental difficulties. On the other hand, the great complexity in AHSS in terms of microstructure and deformation micromechanisms also brings new challenges for understanding HE mechanisms. In this section, we first overview two HE investigations carried out on two representative AHSS classes (DP [11] and medium-Mn [13] steels) as examples to highlight the complex HE problems and the investigation challenges. Then we summarize the complexity, critical problems and major challenges of understanding HE mechanisms in AHSS and discuss the future research steps/directions towards this goal.

4.1 *Example 1:* Hydrogen embrittlement in ferrite-martensite dual-phase steels

Ferrite-martensite DP steels are one of the most widely used AHSS in weight-reduced automotive components. The physical metallurgy behind this material class, i.e., the mixture of both strong and ductile phases to achieve a micromechanical composite effect enabling better strength-ductility synergy, represents an important design strategy for AHSS. The high strength level and the presence of martensite make such steels generally prone to HE. Here we overview the related study from Koyama et al. [11], who developed a detailed discussion on the HE mechanisms in such steels based on careful SEM-based post-mortem analysis. In their study, one grade of DP steel with a martensite fraction of 55 vol.% (Fig. 8 (a)) was selected. H pre-charging was performed electrochemically for 1 h, which was deemed to be sufficient to make the sample saturated with H based on the evaluation using the effective diffusion coefficient of H in fresh martensite. It was

found that H affected both damage nucleation and growth. These two regimes were controlled by different phases with distinctly different HE mechanisms. For the crack nucleation regime, H promoted the decohesion of prior-austenite grain boundaries (Figs. 8 (b_1)~(b_3)), which was attributed to the HEDE effect. However, the surrounding ferrite tended to blunt crack propagation by plastic deformation at the nucleated crack tips (Fig. 8 (b_4)). In this case, H could concentrate on the highly strained zones and provide a HELP effect which efficiently promoted crack propagation inside ferrite (as shown from the EBSD results in Figs. 8 (c_1)~(c_3) and schematic diagrams in Figs. 8 (c_4)~(c_8)). The operation of different HE mechanisms in different phases are likely due to their intrinsically different properties and different interactions with H. The very different C content and substructure between ferrite and α'-martensite could significantly influence the strength level thus the crack driving force, the H trapping [99, 100] and subsequent migration upon deformation, and the resulting localized decohesion and plasticity effects [100].

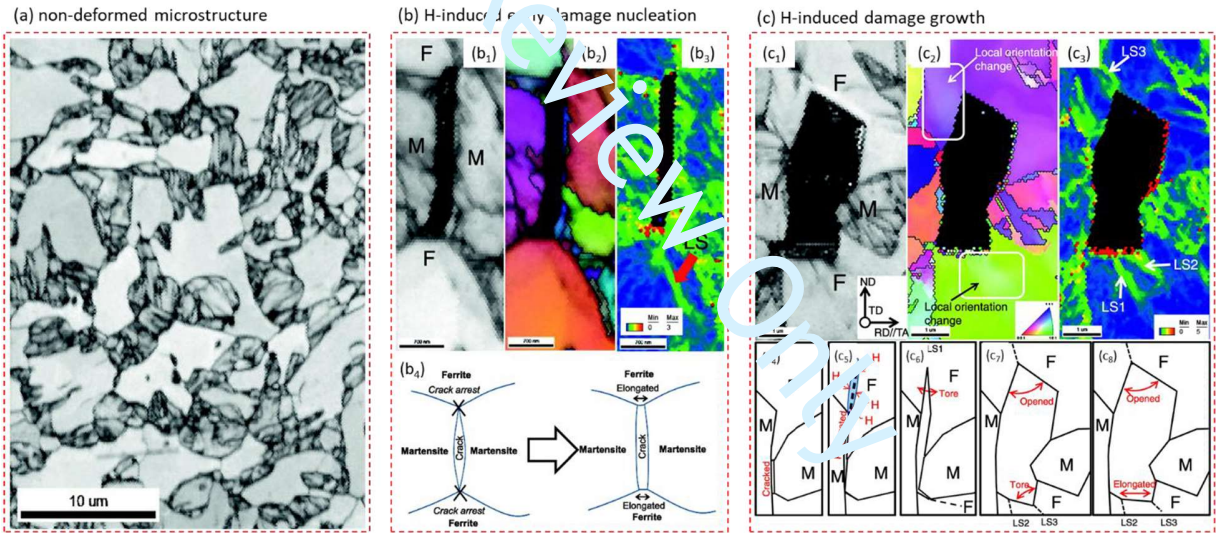

Fig. 8 (a) EBSD image quality (IQ) map showing the initial non-deformed microstructure of the DP steel used in Ref. [11]; (b) EBSD IQ, inverse pole figure (IPF) and Kernel average misorientation (KAM) map (b_1~b_3) and schematic diagrams (b_4) showing the H-induced crack nucleation at prior-austenite grain boundaries, which was proposed to be due to the HEDE effect (c) EBSD results (c_1~c_3) and schematic diagrams (c_4~c_8) showing the H-induced crack propagation inside ferrite close to the crack tip. (Reconstructed with permission from Ref. [11]).

4.2 *Example 2:* Hydrogen embrittlement in ferrite-austenite TRIP-aided medium-Mn steels

Unlike DP steels with a body-centered cubic (bcc) and body-centered tetragonal (bct) structure where H diffusion is relatively fast (diffusion coefficient above 10^{-12} m^2/s at room temperature [101]) thus H saturation within the microstructure can be readily achieved, steels with certain fraction of austenite are difficult to be saturated with H. Based on the reported H diffusion coefficient ($D=10^{-15}$~10^{-13} m^2/s [102]) in duplex stainless steels with around 40~50% austenite, the diffusion distance ($\sim(Dt)^{0.5}$) of H at room temperature after 10 days is only about 30~300 μm. The strong contrast between austenite and ferritic phases in terms of H diffusivity and solubility is likely to result in a heterogeneous H distribution. An extreme case occurs when the austenite fraction is relatively low and the H diffusion is governed by percolating ferrite. In this case, the amount of H trapped inside austenite could be limited given a limited charging time. Such heterogeneous H distribution resulting from a heterogeneous microstructure can significantly affect the active HE mechanisms. In the recent work of Sun et al. [13], two types of ferrite-austenite medium-Mn steels were studied using TDS and careful post-mortem damage analysis. One steel had a ferrite matrix (~75 vol.% α) with austenite islands embedded (Fig. 9 (a)), and the other had an austenite matrix (Fig. 9 (b)). Both steel samples were electrochemically charged for 24h. The fully connected three-dimensional ferritic network in the first sample was deemed to provide a fast path for H transport and the austenite islands can be circumvented by H. This suggested that H was mainly trapped at dislocations and grain boundaries inside ferrite, which was supported by the appearance of only one TDS peak and the associated relatively low H desorption activation energy (E_A=20 kJ/mol, Fig. 9 (a)). The segregated H at dislocations provided a HELP effect, which increased the strain incompatibility between ferrite and neighboring phases thus promoting void nucleation [13]. The dominance of the HELP mechanism in this sample was supported by a dramatically increased (up to ~13 times) void nucleation rate by H, the fracture surface and damage analysis, and the insensitivity of HE resistance to applied strain rates [13]. In contrast for the sample with an austenite matrix, the percolating austenite phase interrupted the efficient diffusion path in ferrite as such H inevitably diffused through the interphase boundaries and austenite and got trapped there. This trapping behavior was supported by the existence of three major peaks in the TDS spectrum and the higher H desorption activation energy for the two higher-temperature peaks (E_A=40 kJ/mol and 51 kJ/mol, Fig. 9 (b)). In this case, the HE was mainly governed by the HEDE mechanism. The initially trapped H at the ferrite-austenite interfaces along with phase transformation-induced H migration to such interface and prior-austenite grain boundaries

decreased their cohesive strength and promoted intergranular cracking [13]. This study again demonstrates that different phase and microstructure constituents in AHSS react differently with H thus showing different embrittlement mechanisms. More importantly, it shows that the initial H distribution and its subsequent migration can greatly affect which phase and the associated HE mechanism is dominant during the failure process.

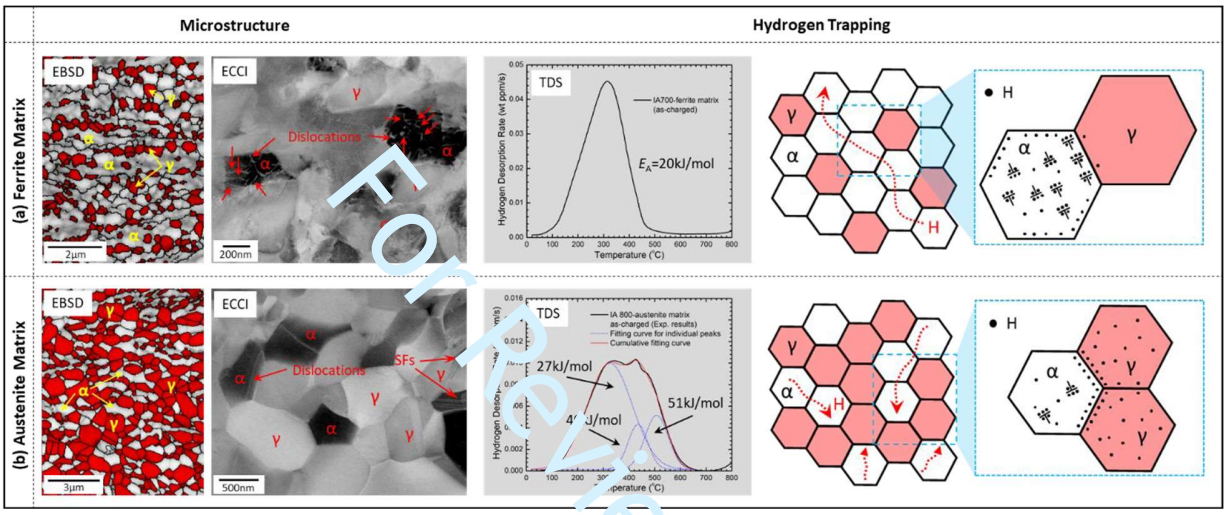

Fig. 9 EBSD and ECCI results, TDS spectrum and schematic diagrams showing the H trapping behavior in a medium-Mn steel with (a) a ferrite matrix and (b) an austenite matrix. (Reconstructed with permission from [13]).

4.3 Challenges of revealing hydrogen embrittlement in AHSS

The above overviewed two studies have shown great complexities of the HE problem in AHSS, especially pertaining to the activation and prevalence of fundamental mechanisms. It is important to mention that despite systematic and careful experiments conducted in these two studies, the proposed HE mechanisms are only supported by indirect evidence without quantitative and precise direct proof. Significant research efforts thus need to be spent in the future in order to fully understand HE in such complex materials. From the authors' point of view, three major challenges exist in this field, which are described in Fig. 10 and listed as follows.

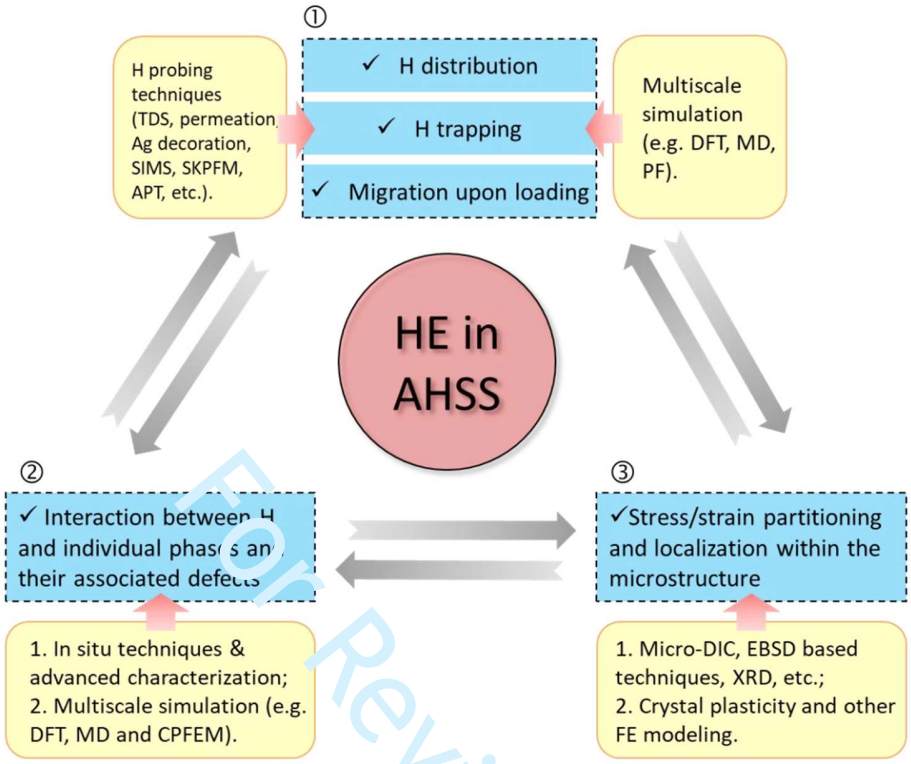

Fig. 10 Schematic diagram showing the major challenges for understanding HE mechanisms in AHSS and common experimental and modeling methods that can be applied to address these challenges.

1. **H distribution, trapping and migration upon loading.** It is well established that the small H atoms can interact with almost all defects in metals. Its local distribution, atomic trapping and migration upon loading are thus vital for the activation of specific HE mechanisms thus the local/global HE resistance. Compared with single-phase model alloys, AHSS have a much more complex microstructure both in non-deformed and deformed states, containing normally multiphases and multiple types of lattice defects [24, 103]. Further, the deformation-driven evolution of microstructure, local stress states and defects are also rather complex and has a significant impact on the local thermodynamics and kinetics of H migration and redistribution. For example, the austenite-to-martensite (α' type) transformation essentially makes the H atoms transfer from an initial low-mobility solute state to a super-saturated and highly mobile state [104-106]. Therefore, without a proper understanding of H trapping and its migration upon loading, any proposed HE mechanisms would seem speculative. This information is especially important when

H is not saturated within the whole sample (as shown in Example 2 in Section 4.2), which is often the case for the H-induced failure in real applications. Therefore, H probing to acquire the microstructure-specific H distribution and its evolution upon loading would be considered as the first critical step to understand HE in AHSS (Fig. 10). Current experimental techniques for probing H include TDS, silver decoration, scanning Kelvin probe force microscopy (SKPFM), secondary ion mass spectroscopy (SIMS), atom probe tomography (APT), neutron radiography, etc. More details regarding these techniques have been overviewed in Ref. [107]. These experimental methods, however, suffer either the lack of spatial resolution (e.g. TDS), or the lack of temporal resolution (e.g. TDS and APT), or incapability of quantification (e.g. Ag decoration and SKPFM), or significant experimental difficulty (e.g. APT). Therefore, significant research efforts are still in high demand to further advance H probing techniques. Various modeling methods such as DFT, molecular dynamics (MD) and phase-field (PF) methods also need to be combined in order to provide more theoretical foundations regarding H behavior in such materials.

2. **Interaction between H and individual phases and their associated defects.** Different phases in AHSS normally have a large difference in terms of mechanical property, defects evolution upon loading, and H solubility and diffusivity. Such intrinsic difference triggers a different H interaction with individual phases and thus different HE mechanisms, as shown in Example 1 described in Section 4.1. Therefore, the H effects on different phases need to be separately treated and investigated. Their respective contribution to the macroscopic H-induced failure also requires a critical assessment. Moreover, the presence of multiple phases essentially produce different types of interphase boundaries [108, 109]. These hetero-interfaces differ from grain boundaries in terms of the interfacial energy as well as the stress/strain field around the interface [109]. Their interaction with H has not been deeply studied from both experimental and modeling perspectives. The aforementioned micromechanical testing methods in combination with *in-situ* H-charging and multiscale simulations (e.g. DFT, MD, PF and crystal plasticity finite element method (CPFEM)) can provide important insights in this field (Fig. 10).

3. **Stress/strain partitioning and localization within the microstructure.** A high degree of strain/stress partitioning and localization is developed in many AHSS upon loading, resulting from their heterogeneous microstructure and the high mechanical contrast among different phases [24,

25, 110-112]. Further, such local strain/stress states can also be dynamically changed or even altered with plasticity deformation that triggers different deformation mechanisms and strain hardening in different phases. For example, Latypov et al. [23] have found that the high strain-hardening capability of retained austenite in a TRIP and TWIP aided medium -Mn steel led to a shift of strain localization initially in austenite to the ferrite phase at later deformation regime. The local strain/stress states and their evolution upon deformation would essentially alter H trapping and migration as well as the local mechanical driving force for damage formation. Such information is thus important to probe, which can be realized by microscale digital image correlation (micro-DIC) [113, 114], X-ray and neutron diffraction [108, 109, 115] and EBSD-based techniques [22] and supported by various modeling methods (e.g. finite element (FE) methods).

5. Summary

This overview discussed the current challenges and opportunities towards understanding HE mechanisms in AHSS. The realization of this task first relies on the accuracy of fundamental HE models proposed in simple model materials, which are still highly debatable. In addition to this point, three other critical questions need be addressed to achieve a full understanding, namely, (a) the H distribution, trapping and migration upon loading, (b) the interaction between H and individual phases and their associated defects, and (c) stress/strain partitioning and localization within the microstructure. The significant influence of the first two points on the prevalent HE mechanisms were reflected from the overviewed HE study in DP steels and medium-Mn steels. The current developed micromechanical testing techniques in combination with *in-situ* H charging can address some of the above challenges. However, much more research efforts on both experiments and multiscale modelling still need to be carried out. Despite great challenges for understanding fundamental HE mechanisms in AHSS, the strategies of mitigating HE susceptibility in such materials are relatively straightforward [5]. Since the occurrence of HE critically depends on the amount of H and their diffusion within the microstructure regardless of specific HE mechanisms, preventing H ingress and introducing deep traps to reduce H diffusivity are generally effective. Based on this, many methods such as the application of protective coatings and the introduction of V- or Ti-based carbides have been developed [5, 15]. The other strategy lies in improving the intrinsic toughness of the material, such as by producing low-energy

interfaces [116] or introducing tough phases [117]. The high toughness of these interfaces or phases can suppress the propagation of H-induced cracks thus improving the HE resistance. These two strategies can thus serve as guidelines for designing new H-resistant AHSS.

6. Reference:

[1] W.H. Johnson, II. On some remarkable changes produced in iron and steel by the action of hydrogen and acids, Proceedings of the Royal Society of London 23 (1875) 168-179.
[2] R.P. Gangloff, B.P. Somerday. Gaseous hydrogen embrittlement of materials in energy technologies: the problem, its characterisation and effects on particular alloy classes: Elsevier, 2012.
[3] X. Lu, D. Wang, Effect of hydrogen on deformation behavior of Alloy 725 revealed by in-situ bi-crystalline micropillar compression test, Journal of Materials Science & Technology (2020).
[4] A. Alvaro, et al., Hydrogen embrittlement in nickel, visited by first principles modeling, cohesive zone simulation and nanomechanical testing, international journal of hydrogen energy 40 (2015) 16892-16900.
[5] H.K.D.H. Bhadeshia, Prevention of hydrogen embrittlement in steels, ISIJ Int. 56 (2016) 24-36.
[6] Y. Deng, A. Barnoush, Hydrogen embrittlement revealed via novel in situ fracture experiments using notched micro-cantilever specimens, Acta Materialia 142 (2018) 236-247.
[7] M. Koyama, et al., Overview of hydrogen embrittlement in high-Mn steels, international journal of hydrogen energy 42 (2017) 12706-12723.
[8] M.L. Martin, et al., Enumeration of the hydrogen-enhanced localized plasticity mechanism for hydrogen embrittlement in structural materials, Acta Materialia (2018).
[9] I. Robertson, et al., Hydrogen effects on plasticity, Dislocations in solids 15 (2009) 249-293.
[10] A.J. Breen, et al., Solute hydrogen and deuterium observed at the near atomic scale in high-strength steel, Acta Materialia 188 (2020) 108-120.
[11] M. Koyama, et al., Hydrogen-assisted decohesion and localized plasticity in dual-phase steel, Acta Materialia 70 (2014) 174-187.
[12] Q. Liu, et al., A review of the influence of hydrogen on the mechanical properties of DP, TRIP, and TWIP advanced high-strength steels for auto construction, Corrosion Reviews 34 (2016) 127-152.
[13] B. Sun, et al., Dependence of hydrogen embrittlement mechanisms on microstructure-driven hydrogen distribution in medium Mn steels, Acta Materialia 183 (2020) 313-328.
[14] J. Han, et al., The mechanism of hydrogen embrittlement in intercritically annealed medium Mn TRIP steel, Acta Materialia 113 (2016) 1-10.
[15] O. Barrera, et al., Understanding and mitigating hydrogen embrittlement of steels: a review of experimental, modelling and design progress from atomistic to continuum, Journal of materials science 53 (2018) 6251-6290.
[16] S. Lynch, Hydrogen embrittlement phenomena and mechanisms, Corrosion Reviews 30 (2012) 105-123.
[17] C. McMahon Jr, Hydrogen-induced intergranular fracture of steels, Engineering Fracture Mechanics 68 (2001) 773-788.
[18] M.B. Djukic, et al., The synergistic action and interplay of hydrogen embrittlement mechanisms in steels and iron: Localized plasticity and decohesion, Engineering Fracture Mechanics 216 (2019) 106528.
[19] M. Nagumo, K. Takai, The predominant role of strain-induced vacancies in hydrogen embrittlement of steels: overview, Acta Materialia (2018).
[20] S. Lynch. Hydrogen embrittlement (HE) phenomena and mechanisms. Stress Corrosion Cracking. Elsevier, 2011. p.90-130.
[21] R. Kirchheim, Revisiting hydrogen embrittlement models and hydrogen-induced homogeneous nucleation of dislocations, Scripta materialia 62 (2010) 67-70.

[22] D. An, et al., Direct observations of collinear dislocation interaction in a Fe-17.4 Mn-1.50 Al-0.29 C (wt.%) austenitic steel under cyclic loading by in-situ electron channelling contrast imaging and cross-correlation electron backscatter diffraction, Scripta Materialia 186 (2020) 341-345.
[23] M.I. Latypov, et al., Micromechanical finite element analysis of strain partitioning in multiphase medium manganese TWIP+ TRIP steel, Acta Materialia 108 (2016) 219-228.
[24] D. Raabe, et al., Current challenges and opportunities in microstructure-related properties of Advanced High-Strength Steels, Metallurgical and Materials Transactions A 51 (2020) 5517-5586.
[25] B. Sun, et al., The influence of silicon additions on the deformation behavior of austenite-ferrite duplex medium manganese steels, Acta Materialia 148 (2018) 249-262.
[26] B. Sun, et al., Phase transformation behavior of medium manganese steels with 3 wt pct aluminum and 3 wt pct silicon during intercritical annealing, Metallurgical and Materials Transactions A 47 (2016) 4869-4882.
[27] B. Sun, et al., Improving the ductility of ultrahigh-strength medium Mn steels via introducing pre-existed austenite acting as a "reservoir" for Mn atoms, Materials Science and Engineering: A 749 (2019) 235-240.
[28] R. Oriani, A mechanistic theory of hydrogen embrittlement of steels, Berichte der Bunsengesellschaft für physikalische Chemie 76 (1972) 848-857.
[29] A.R. Troiano, The role of hydrogen and other interstitials in the mechanical behavior of metals, Metallography, Microstructure, and Analysis 5 (2016) 557-569.
[30] T. Perng, C. Altstetter, Comparison of hydrogen gas embrittlement of austenitic and ferritic stainless steels, Metallurgical Transactions A 18 (1987) 123-134.
[31] W.W. Gerberich, et al., The necessity of both plasticity and brittleness in the fracture thresholds of iron, Philosophical Magazine A 63 (1991) 363-376.
[32] M. Yamaguchi, et al., Mobile effect of hydrogen on intergranular decohesion of iron: first-principles calculations, Philosophical Magazine 92 (2012) 1349-1368.
[33] G.A. Young, J.R. Scully. Hydrogen production, absorption and transport during environment assisted cracking of an Al-Zn-Mg-(Cu) alloy in humid air. International Conference on Hydrogen Effects on Material Behavior and Corrosion Deformation Interactions, Moran, WY, 2002. p.22-26.
[34] D. Li, et al., Hydrogen trap states in ultrahigh-strength AERMET 100 steel, Metallurgical and materials transactions A 35 (2004) 849-864.
[35] J. Song, W. Curtin, A nanoscale mechanism of hydrogen embrittlement in metals, Acta Materialia 59 (2011) 1557-1569.
[36] M. Seah, Adsorption-induced interface decohesion, Acta Metallurgica 28 (1980) 955-962.
[37] B. Sun, et al., Revealing fracture mechanisms of medium manganese steels with and without delta-ferrite, Acta Materialia 164 (2019) 683-696.
[38] D. Jiang, E.A. Carter, First principles assessment of ideal fracture energies of materials with mobile impurities: implications for hydrogen embrittlement of metals, Acta materialia 52 (2004) 4801-4807.
[39] R. Matsumoto, et al., Atomistic simulations of hydrogen embrittlement, International Journal of Hydrogen Energy 34 (2009) 9576-9584.
[40] A. Tahir, et al., Hydrogen embrittlement of a carbon segregated Σ5 (310)[001] symmetrical tilt grain boundary in α-Fe, Materials Science and Engineering: A 612 (2014) 462-467.
[41] C.D. Beachem, A new model for hydrogen-assisted cracking (hydrogen "embrittlement"), Metallurgical and Materials Transactions B 3 (1972) 441-455.
[42] H.K. Birnbaum, P. Sofronis, Hydrogen-enhanced localized plasticity—a mechanism for hydrogen-related fracture, Materials Science and Engineering: A 176 (1994) 191-202.
[43] P. Sofronis, H.K. Birnbaum, Mechanics of the hydrogendashdislocationdashimpurity interactions—I. Increasing shear modulus, Journal of the Mechanics and Physics of Solids 43 (1995) 49-90.
[44] S. Wang, et al., Hydrogen-induced change in core structures of {110}[111] edge and {110}[111] screw dislocations in iron, Scientific reports 3 (2013) 1-4.

[45] M. Itakura, et al., The effect of hydrogen atoms on the screw dislocation mobility in bcc iron: a first-principles study, Acta materialia 61 (2013) 6857-6867.
[46] J. Song, W. Curtin, Mechanisms of hydrogen-enhanced localized plasticity: an atomistic study using α-Fe as a model system, Acta Materialia 68 (2014) 61-69.
[47] J. Song, W. Curtin, Atomic mechanism and prediction of hydrogen embrittlement in iron, Nature materials 12 (2013) 145-151.
[48] D. Xie, et al., Hydrogenated vacancies lock dislocations in aluminium, Nature communications 7 (2016) 1-7.
[49] P. Ferreira, et al., Hydrogen effects on the interaction between dislocations, Acta materialia 46 (1998) 1749-1757.
[50] D. Shih, et al., Hydrogen embrittlement of α titanium: in situ TEM studies, Acta Metallurgica 36 (1988) 111-124.
[51] T. Tabata, H. Birnbaum, Direct observations of the effect of hydrogen on the behavior of dislocations in iron, Scripta Metallurgica 17 (1983) 947-950.
[52] K. Christmann, Some general aspects of hydrogen chemisorption on metal surfaces, Progress in surface science 48 (1995) 15-26.
[53] P. Ferrin, et al., Hydrogen adsorption, absorption and diffusion on and in transition metal surfaces: A DFT study, Surface science 606 (2012) 679-689.
[54] H. Johnson. Hydrogen gas embrittlement. Cornell Univ., Ithaca, NY (USA), 1973.
[55] M. Nagumo, et al., Deformation induced defects in iron revealed by thermal desorption spectroscopy of tritium, Scripta materialia 40 (1999).
[56] M. Nagumo, Hydrogen related failure of steels–a new aspect, Materials Science and Technology 20 (2004) 940-950.
[57] M. Nagumo, et al., Hydrogen thermal desorption relevant to delayed-fracture susceptibility of high-strength steels, Metallurgical and Materials Transactions A 32 (2001) 339-347.
[58] M. Nagumo, K. Takai, The predominant role of strain-induced vacancies in hydrogen embrittlement of steels: overview, Acta Materialia 165 (2019) 722-733.
[59] K. Sakaki, et al., The effect of hydrogen on vacancy generation in iron by plastic deformation, Scripta Materialia 55 (2006) 1031-1034.
[60] R. Kirchheim, On the solute-defect interaction in the framework of a defactant concept, International journal of materials research 100 (2009) 483-487.
[61] T. Neeraj, et al., Hydrogen embrittlement of ferritic steels: observations on deformation microstructure, nanoscale dimples and failure by nanovoiding, Acta Materialia 60 (2012) 5160-5171.
[62] R. Kirchheim, Reducing grain boundary, dislocation line and vacancy formation energies by solute segregation. I. Theoretical background, Acta Materialia 55 (2007) 5129-5138.
[63] R. Kirchheim, Reducing grain boundary, dislocation line and vacancy formation energies by solute segregation: II. Experimental evidence and consequences, acta materialia 55 (2007) 5139-5148.
[64] D. Wang, et al., Effect of hydrogen on nanomechanical properties in Fe-22Mn-0.6C TWIP steel revealed by in-situ electrochemical nanoindentation, Acta Mater. 166 (2019) 618-629.
[65] A. Barnoush, H. Vehoff, Recent developments in the study of hydrogen embrittlement: Hydrogen effect on dislocation nucleation, Acta Materialia 58 (2010) 5274-5285.
[66] C. Zapffe, C. Sims, Hydrogen embrittlement, internal stress and defects in steel, Trans. AIME 145 (1941) 225-271.
[67] R. Oriani, Hydrogen embrittlement of steels, Annual review of materials science 8 (1978) 327-357.
[68] Y. Chang, et al., Ti and its alloys as examples of cryogenic focused ion beam milling of environmentally-sensitive materials, Nature communications 10 (2019) 1-10.
[69] I. Gutierrez-Urrutia, et al., Plastic accommodation at homophase interfaces between nanotwinned and recrystallized grains in an austenitic duplex-microstructured steel, Sci Technol Adv Mater 17 (2016) 29-36.
[70] J. Zhang, et al., Designing duplex, ultrafine-grained Fe-Mn-Al-C steels by tuning phase transformation and recrystallization kinetics, Acta Mater. 141 (2017) 374-387.

[71] D. Yan, et al., High resolution in situ mapping of microstrain and microstructure evolution reveals damage resistance criteria in dual phase steels, Acta Mater. 96 (2015) 399-409.
[72] J. Nellessen, et al., Effects of strain amplitude, cycle number and orientation on low cycle fatigue microstructures in austenitic stainless steel studied by electron channelling contrast imaging, Acta Mater. 87 (2015) 86-99.
[73] X. Lu, et al., Effect of electrochemical charging on the hydrogen embrittlement susceptibility of Alloy 718, Acta Mater. 179 (2019) 36-48.
[74] T. Depover, et al., The effect of hydrogen on the crack initiation site of TRIP-assisted steels during in-situ hydrogen plasma micro-tensile testing: Leading to an improved ductility?, Mater. Charact. 167 (2020).
[75] D. Wang, et al., Effect of hydrogen on the embrittlement susceptibility of Fe-22Mn-0.6C TWIP steel revealed by in-situ tensile tests, Mater. Sci. Eng. A (2020) 140638.
[76] M. Koyama, et al., Origin of micrometer-scale dislocation motion during hydrogen desorption, Science Advances 6 (2020) eaaz1187.
[77] A. Massone, et al., An SEM compatible plasma cell for in situ studies of hydrogen-material interaction, Rev. Sci. Instrum. 91 (2020) 043705.
[78] J. Kim, C.C. Tasan, Microstructural and micro-mechanical characterization during hydrogen charging: An in situ scanning electron microscopy study, International Journal of Hydrogen Energy 44 (2019) 6333-6343.
[79] D. Wan, et al., Hydrogen-enhanced fatigue crack growth in a single-edge notched tensile specimen under in-situ hydrogen charging inside an environmental scanning electron microscope, Acta Materialia 170 (2019) 87-99.
[80] N.G. Chechenin, et al., Nanoindentation of amorphous aluminum oxide films II. Critical parameters for the breakthrough and a membrane effect in thin hard films on soft substrates, Thin Solid Films 261 (1995) 228-235.
[81] D. Beegan, et al., Comparison between nanoindentation and scratch test hardness (scratch hardness) values of copper thin films on oxidised silicon substrates, Surf. Coat. Technol. 201 (2007) 5804-5808.
[82] W.C. Oliver, G.M. Pharr, Measurement of hardness and elastic modulus by instrumented indentation: Advances in understanding and refinements to methodology, J. Mater. Res. 19 (2004) 3-20.
[83] D.K. Han, et al., Hydrogen and aluminium in high-manganese twinning-induced plasticity steel, Scr. Mater. 80 (2014) 9-12.
[84] Y. Zhao, et al., Hydrogen-induced nanohardness variations in a CoCrFeMnNi high-entropy alloy, Int. J. Hydrog. Energy 42 (2017) 12015-12021.
[85] T. Depover, et al., Assessment of the potential of hydrogen plasma charging as compared to conventional electrochemical hydrogen charging on dual phase steel, Mater. Sci. Eng. A 754 (2019) 613-621.
[86] A.S. Ebner, et al., A Modified Electrochemical Nanoindentation Setup for Probing Hydrogen-Material Interaction Demonstrated on a Nickel-Based Alloy, Jom (2020).
[87] N. Kheradmand, et al., Effect of hydrogen on the hardness of different phases in super duplex stainless steel, Int. J. Hydrog. Energy 41 (2016) 704-712.
[88] M. Asgari, et al., Nanomechanical characterization of the hydrogen effect on pulsed plasma nitrided super duplex stainless steel, Int. J. Hydrog. Energy 38 (2013) 15520-15531.
[89] X. Lu, et al., Insight into hydrogen effect on a duplex medium-Mn steel revealed by in-situ nanoindentation test, Int. J. Hydrog. Energy 44 (2019) 20545-20551.
[90] D. Wang, et al., In-situ observation of martensitic transformation in an interstitial metastable high-entropy alloy during cathodic hydrogen charging, Scripta Materialia 173 (2019) 56-60.
[91] D. Wang, et al., Effect of hydrogen-induced surface steps on the nanomechanical behavior of a CoCrFeMnNi high-entropy alloy revealed by in-situ electrochemical nanoindentation, Intermetallics 114 (2019) 106605.
[92] Y. Deng, et al., In-situ micro-cantilever bending test in environmental scanning electron microscope: Real time observation of hydrogen enhanced cracking, Scr. Mater. 127 (2017) 19-23.

[93] X. Lu, et al., Hydrogen susceptibility of an interstitial equimolar high-entropy alloy revealed by in-situ electrochemical microcantilever bending test, Mater. Sci. Eng. A 762 (2019) 138114.
[94] X. Lu, et al., On the hydrogen embrittlement behavior of nickel-based alloys: Alloys 718 and 725, Mater. Sci. Eng. A 792 (2020) 139785.
[95] D. Wan, et al., Hydrogen embrittlement effect observed by in-situ hydrogen plasma charging on a ferritic alloy, Scripta Materialia 151 (2018) 24-27.
[96] B.R.S. Rogne, et al., In situ micromechanical testing in environmental scanning electron microscope: A new insight into hydrogen-assisted cracking, Acta Mater. 144 (2018) 257-268.
[97] J. Venezuela, et al., A review of hydrogen embrittlement of martensitic advanced high-strength steels, Corrosion Reviews 34 (2016) 153-186.
[98] C.C. Tasan, et al., An overview of dual-phase steels: advances in microstructure-oriented processing and micromechanically guided design, Annual Review of Materials Research 45 (2015) 391-431.
[99] A. Turk, et al., Quantification of hydrogen trapping in multiphase steels: Part I–Point traps in martensite, Acta Materialia 194 (2020) 118-133.
[100] W. Geng, et al., Hydrogen trapping in carbon supersaturated α-iron and its decohesion effect in martensitic steel, Scripta Materialia 149 (2018) 79-83.
[101] J. Sun, et al., A lamellar structured ultrafine grain ferrite-martensite dual-phase steel and its resistance to hydrogen embrittlement, Journal of Alloys and Compounds 698 (2017) 390-399.
[102] V. Olden, et al., FE simulation of hydrogen diffusion in duplex stainless steel, International journal of hydrogen energy 39 (2014) 1156-1163.
[103] B. Sun, et al., Discontinuous strain-induced martensite transformation related to the Portevin-Le Chatelier effect in a medium manganese steel, Scripta Materialia 133 (2017) 9-13.
[104] M. Koyama, et al., Martensitic transformation-induced hydrogen desorption characterized by utilizing cryogenic thermal desorption spectroscopy during cooling, Scripta Materialia 122 (2016) 50-53.
[105] T. Hojo, et al., Transformation-assisted hydrogen desorption during deformation in steels: Examples of α′-and ε-Martensite, International Journal of Hydrogen Energy 44 (2019) 30472-30477.
[106] J.H. Ryu, et al., Effect of deformation on hydrogen trapping and effusion in TRIP-assisted steel, Acta materialia 60 (2012) 4085-4092.
[107] M. Koyama, et al., Recent progress in microstructural hydrogen mapping in steels: quantification, kinetic analysis, and multi-scale characterisation, Materials Science and Technology 33 (2017) 1481-1496.
[108] B. Sun, et al., Macroscopic to nanoscopic in situ investigation on yielding mechanisms in ultrafine grained medium Mn steels: Role of the austenite-ferrite interface, Acta Materialia 178 (2019) 10-25.
[109] Y. Ma, et al., Phase boundary segregation-induced strengthening and discontinuous yielding in ultrafine-grained duplex medium-Mn steels, Acta Materialia 200 (2020) 389-403.
[110] B. Sun, et al., Critical role of strain partitioning and deformation twinning on cracking phenomenon occurring during cold rolling of two duplex medium manganese steels, Scripta Materialia 130 (2017) 49-53.
[111] B. Sun, et al., Microstructure evolution of a medium manganese steel during thermomechanical processing, Metallurgical and Materials Transactions A 47 (2016) 1782-1791.
[112] B. Sun, et al., Microstructural characteristics and tensile behavior of medium manganese steels with different manganese additions, Materials Science and Engineering: A 729 (2018) 496-507.
[113] A. Dutta, et al., Strain partitioning and strain localization in medium manganese steels measured by in situ microscopic digital image correlation, Materialia 5 (2019) 100252.
[114] Z. Zhang, et al., Strain localisation and failure at twin-boundary complexions in nickel-based superalloys, Nature communications 11 (2020) 1-11.
[115] P.J. Gibbs, et al., Strain partitioning in ultra-fine grained medium-manganese transformation induced plasticity steel, Materials Science and Engineering: A 609 (2014) 323-333.
[116] S. Bechtle, et al., Grain-boundary engineering markedly reduces susceptibility to intergranular hydrogen embrittlement in metallic materials, Acta materialia 57 (2009) 4148-4157.

[117] M. Wang, et al., Enhancing hydrogen embrittlement resistance of lath martensite by introducing nano-films of interlath austenite, Metallurgical and Materials Transactions A 46 (2015) 3797-3802.